**Aalborg Universitet**

AALBORG UNIVERSITY
DENMARK

**Reliability Analysis of Geotechnical Failure Modes for Vertical Wall Breakwaters**

Sørensen, John Dalsgaard; Burcharth, H. F.

# Reliability analysis of geotechnical failure modes for vertical wall breakwaters

John Dalsgaard Sørensen *, Hans F. Burcharth

*Aalborg University, Sohngaardsholmsvej 57, DK-9000 Aalborg, Denmark*

## 1. Introduction

Vertical wall breakwaters are usually designed as concrete caissons placed on the top of a rubble mound foundation or a rubble bedding layer. The purpose of the breakwater is usually to protect the area behind the breakwater from being flooded by large waves. The area protected can for example be a harbour of small or large importance, an important industrial area or a heavily populated coast line. This implies that vertical wall breakwaters are used under quite different conditions and therefore the consequences of a complete or partial failure also are very different. This implies that the accepted probability of failure also varies considerably which also can be observed from the actual observed failure rates.

A number of different failure modes are relevant to consider for vertical wall breakwaters (e.g. [1]). Foundation failure modes include sliding of the breakwater relative to the rubble mound and different foundation failure modes with failure within the rubble mound and the subsoil (sand or clay). Hydraulic failure modes include wave overtopping, wave transmission and wave reflection. Structural failure modes involve failure or partial failure of the concrete caissons. In this paper only geotechnical failure modes are considered.

In order to estimate the reliability, stochastic models for the uncertain parameters in the limit state functions are formulated. The main horizontal and vertical (uplift) loading on vertical wall breakwaters are wave loads, including both pulsating and impact wave loads. Stochastic models for the wave loading are presented. These

* Corresponding author. Tel.: +45-9635-8581; fax: 45+9814-8243.
  *E-mail address:* i6jds@civil.auc.dk (J.D. Sørensen).

load models are partly based on laboratory tests. Therefore the related statistical and model uncertainties are included. Further stochastic models for the soil strength parameters are formulated. These models are based on the site specific information usually available and engineering judgment (prior information) and are formulated in such a way that updating using Bayesian statistics is possible.

In this paper limit state functions are formulated for a number of possible geotechnical failure modes. The limit state functions are described using the upper bound theory of general plasticity theory assuming kinematically possible failure mechanisms. It is shown how the most critical failure modes can be modeled in a limit state function by minimizing the total virtual work with respect to the free parameters modeling the failure modes. As an example a reliability analysis is performed for the geotechnical failure modes for the Niigata West breakwater in Japan.

## 2. Failure modes

In Fig. 2 a typical vertical wall breakwater is shown. The following groups of geotechnical failure modes shown in Fig. 1 should be considered when analyzing vertical wall breakwaters [1–4]:

- sliding between bottom of caisson and top of rubble mound
- slip failure in rubble mound
- slip failure in rubble mound and sand subsoil
- slip failure in rubble mound and clay subsoil

## 3. Stochastic models

### 3.1. Wave load

The main load for vertical wall structures is due to wave loading. Depending on the geometry of the rubble mound and the caisson the wave loading can be characterized as (e.g. [5]):

- Quasi-static (pulsating) wave load which can be estimated using the Goda formula, [6]. The horizontal and the vertical wave pressure, see (Fig. 3), can be determined as a function of the significant wave height $H_S$ at deep water.
- Impact loading characterized by a very high load but with a very short duration. The impact loading which consists of a horizontal and a vertical (uplift) part can be estimated by the model in [5] or by an extension of the Goda formulae [7]. In this paper, impact loading is not considered explicitly and the possible undrained behavior of the rubble mound material and the sand subsoil is not taken into account.
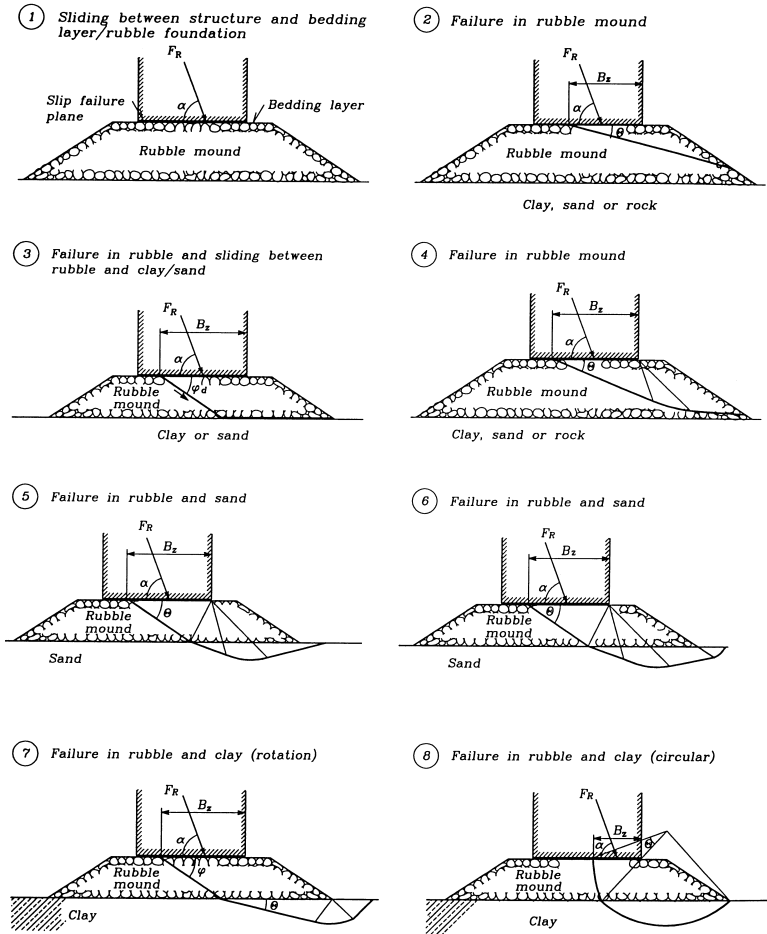
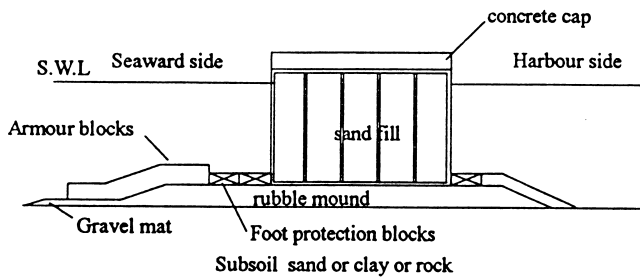Fig. 1. Geotechnical failure modes.



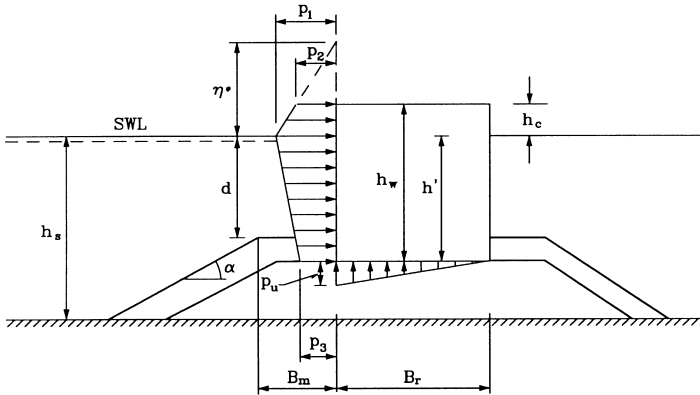Fig. 2. Typical vertical wall breakwater in shallow water.

Fig. 3. Wave induced quasi-static load according to Goda [6].

## 3.2. Wave height

The maximum significant wave height $H_S^T$ in the design lifetime $T$ usually has to be modeled on the basis of a limited number $N$ of wave height observations. Here an extreme Weibull distribution is used [8]:

$$F_{H_S^T}(h) = \left[ 1 - \exp\left( -\left( \frac{h - H'}{u} \right)^\alpha \right) \right]^{\lambda T} \tag{1}$$

where $\lambda$ is the number of observations per year. $\alpha$, $u$ and $H'$ are parameters to be fitted to the observed data. In order to model the statistical uncertainty $u$ is modeled as a Normally distributed stochastic variable with coefficient of variation $V_u = \frac{1}{\sqrt{N}} \sqrt{\frac{\Gamma(1+2/\alpha)}{\Gamma^2(1+1/\alpha)} - 1}$. The model uncertainty related to the quality of the measured wave data is modeled by a multiplicative stochastic variable $U_{H_S}$ which is assumed to be Normally distributed with expected value 1 and standard deviation equal to 0.05 or 0.2 corresponding to good or poor wave data. Further, the water level set-up due to storm wind and waves (storm surge) is difficult to estimate except for simple conditions (straight coastline and constant slope of sea bed). The uncertainty related to storm surge varies considerably with the environmental conditions. In the reliability analysis this uncertainty on the storm surge water level is modeled by a stochastic variable with mean zero and standard deviation equal to $0.05H_S$.

## 3.3. Geotechnical parameters

In general, the material characteristics of the soil have to be modeled as a stochastic field. The parameters describing the stochastic field have to be determined on the basis of the measurements which are usually performed to characterize the soil characteristics. Since these measurements are only performed in a few points statistical uncertainty due to few data points is also introduced and has to be included in

the statistical model. Further, the uncertainty in the determination of the soil properties and the measurement uncertainty have to be included in the statistical model. In the literature the undrained shear strength of clay is often modeled by a log-Gaussian distributed stochastic field $\{c_u(x, z)\}$ (e.g. [9]). The expected value function $E[c_u(x, z)]$ and the covariance function $C[c_u(x_1, z_1), c_u(x_2, z_2)]$ can typically be written:

$$E[c_u(x, z)] = E[c_u(z)] \tag{2}$$

$$C[c_u(x_1, z_1), c_u(x_2, z_2)] = C[c_u(x_1 - x_2, z_1 - z_2)] \tag{3}$$

where $(x_1, z_1)$ and $(x_2, z_2)$ are two points in the soil. $E[c_u(z)]$ models the expected value of the undrained shear strength in depth $z$. $C[c_u(x_1 - x_2, z_1 - z_2)]$ models the covariance between $c_u$ at position $(x_1, z_1)$ and $c_u$ at position $(x_2, z_2)$. It is seen that the expected value depends on the depth and the covariance depends on the vertical and horizontal distances. Generally, the correlation lengths in horizontal and vertical direction will be different due to the soil stratification.

The statistical parameters describing $E[c_u(z)]$ and $C[c_u(x_1 - x_2, z_1 - z_2)]$ should be modeled using Bayesian statistics such that prior, subjective knowledge on the values of the parameters can be combined with measurements from the actual site (e.g. [10]). In practical calculations the stochastic field is discretized taking into account the correlation lengths of the field. If an integral over some domain is used, the expected value and the standard deviation of this integral can be evaluated numerically as shown in Section 4 below.

Since the breakwater foundation is made of friction material and it is assumed that foundation failure modes can develop both in the rubble mound and in the sand subsoil, statistical models for the effective friction angle and the angle of dilation are needed for the rubble material and the sand subsoil. In this paper these angles are modeled by Lognormal stochastic variables, i.e. the spatial variation is not taken into account.

Model uncertainty connected to the mathematical models for the geotechnical failure modes used to estimate the soil strength can be important due to the relatively high uncertainty related to the models used. If slip failure models based on the upper bound theorem of plasticity theory are used these can be evaluated by comparison with results from more refined numerical calculations using nonlinear finite element programs with realistic constitutive equations implemented for the soil. Estimates of the model uncertainties can then be obtained by comparing the results. The estimates of the model uncertainties should also to some degree depend on professional, subjective insight into the failure modes considered.

As mentioned above, the bearing capacities related to the geotechnical failure modes are in this paper estimated using the upper bound theorem of classical plasticity theory where an associated flow rule is assumed. However, the friction angle and the dilation angle for the rubble mound material and the sand subsoil are usually different. Therefore, in order to use the theory based on an associated flow rule, the following reduced effective friction angle $\varphi_d$ is used [11]:

$$\tan \varphi_d = \frac{\sin \varphi' \cos \psi}{1 - \sin \varphi' \sin \psi} \qquad (4)$$

where $\varphi'$ is the effective friction angle and $\psi$ is the dilation angle.

## 4. Reliability analysis

The failure modes described in Section 2 can be characterized as ultimate limit states and the probability of failure within the design lifetime $T$ can then be estimated by

$$P_f = \Phi(-\beta_S) = P\left(\bigcup_{i=1}^{n}\{g_i(\mathbf{X}) \leqslant 0\}\right) \qquad (5)$$

where $g_i(\mathbf{X})$ is the safety margin for failure mode no $i$ and $\mathbf{X}$ is a vector with the stochastic variables. $\beta_S$ is the system reliability index corresponding to the probability of failure $P_f$ estimated by FORM analysis [12,13]. $\Phi(\cdot)$ is the distribution function for a standard Normally distributed stochastic variable. The probability of failure $P_{f_i}$ for each failure mode is also determined by FORM:

$$P_{f_i} = P(g_i(\mathbf{X}) \leqslant 0) \approx P(\beta_i - \alpha_i^T \mathbf{U} \leqslant 0) = \Phi(-\beta_i) \qquad (6)$$

where $\beta_i$ is the reliability index for failure mode $i$, $\alpha_i$ is a unit vector with elements indicating the relative importance of the stochastic variables and $\mathbf{U}$ is a vector with standardized Normally distributed stochastic variables.

For a given kinematically admissible failure mechanism the internal work for an infinitisimal displacement $\delta = 1$ is denoted by $W_{I,i}(\theta, \mathbf{X})$ where $\theta$ is a vector with the free parameters describing the mechanism. Correspondingly the external work for the infinitisimal displacement is denoted by $W_{E,i}(\theta, \mathbf{X})$.

The limit state function is written

$$g_i(\mathbf{X}) = \min_{\theta}\{W_{I,i}(\theta, \mathbf{X}) - W_{E,i}(\theta, \mathbf{X})\} \qquad (7)$$

where the minimization of $W_{I,i}(\theta, \mathbf{X}) - W_{E,i}(\theta, \mathbf{X})$ is performed with respect to $\theta$. Further, constraints can be added to (6) in order to limit the displacements and to describe the displacements of the failure mechanism.

Ten limit state functions are formulated for the following failure modes:

- sliding:
  1. sliding between caisson and bedding layer/rubble foundation

- failure in rubble mound:
  2. rupture in rubble along bottom of caisson
  3. rupture in rubble mound — straight rupture line
  4. rupture in rubble mound — curved rupture line

- failure in rubble mound and sand subsoil
    5. rupture in subsoil along bottom of rubble mound
    6. rupture in rubble mound and sand subsoil — mode 1
    7. rupture in rubble mound and sand subsoil — mode 2

- failure in rubble mound and clay subsoil
    8. rupture in subsoil along bottom of rubble mound
    9. rupture in rubble mound and sand subsoil — mode 1
    10. rupture in rubble mound and sand subsoil — mode 2

In the following limit state functions are formulated for failure modes 1, 2, 3 and 9. The Appendix contains the limit state functions for the other failure modes.

## 4.1. Sliding between caisson and bedding layer/rubble foundation — failure modes 1 and 2

The failure mechanism consists of horizontal sliding on the bedding layer (see Fig. 4). The limit state function is written:

$$g(\mathbf{X}) = (F_G - F_U)\tan\mu - F_H \tag{8}$$

where:

$F_G$      weight of caisson reduced for buoyancy
$F_U$      wave induced uplift
$F_H$      horizontal wave force
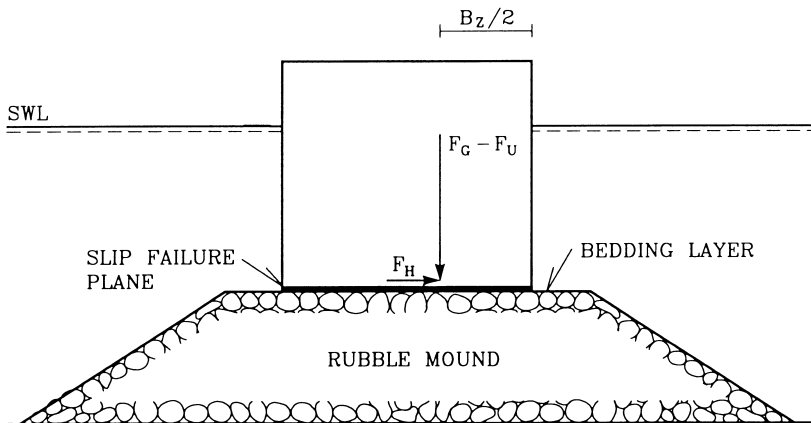


Fig. 4. Sliding failure between caisson and bedding layer/rubble foundation.

$\tan \mu$     = friction coefficient $f$ if sliding occurs between the concrete base plate and the bedding layer (failure mode 1), or

             = $\tan \varphi_{d_1}$ if sliding occurs entirely in the rubble mound (failure mode 2)

$\varphi_{d_1}$        reduced effective angle of friction of the rubble mound

## 4.2. Failure in rubble mound — failure mode 3

The effective width $B_z$ of the caisson is determined such that the resultant vertical force $F_G - F_U$ is placed $B_z/2$ from the heel of the caisson (see Fig. 5). The failure mechanism consists of a unit displacement along the line AB and is described by the angle $\theta$ of the rupture line. The area of zone 1 can be written:

$$A_1 = \frac{1}{2}(B_z + a)^2 (\cos \theta \sin \theta + \sin^2 \theta \tan(\frac{\pi}{2} + \theta - \tan^{-1}(h_{II}/b))) \qquad (9)$$

The limit state function is written

$$g(\mathbf{X}) = \min_{\theta} \left\{ (\gamma_s - \gamma_w)A_1 \omega_{1V} + (F_G - F_U)\omega_{1V} - F_H \omega_{1H} \right\} \qquad (10)$$

where

$F_G$     weight of caisson reduced for buoyancy

$F_U$     wave induced uplift

$F_H$     horizontal wave force

$\gamma_s$      unit weight of rubble material

$\gamma_w$     unit weight of water

$\omega_{1H}$    = $\cos(\varphi_{d_1} - \theta)/\cos(\varphi_{d_1})$ is the horizontal displacement

$\omega_{1V}$    = $\sin(\varphi_{d_1} - \theta)/\cos(\varphi_{d_1})$ is the vertical displacement
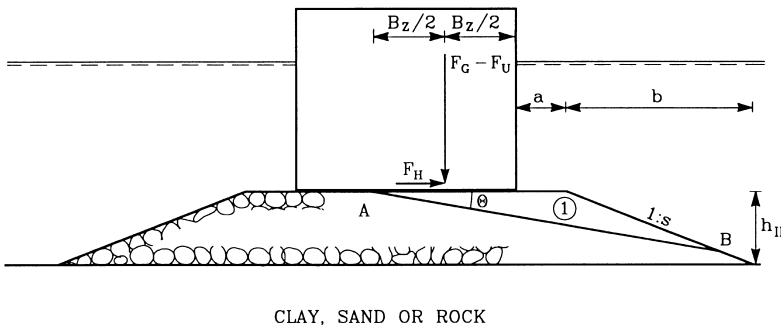


Fig. 5. Failure in rubble mound.

The effect of wave induced pressure along the rupture boundary is added to the horizontal wave force $F_H$. The following constraint is added since the rupture line should be within the rubble mound:

$$0 \leqslant \theta \leqslant \tan^{-1} \left( \frac{h_{II}}{B_z + a + b} \right) \tag{11}$$

### 4.3. Failure in rubble mound and clay subsoil — failure mode 9

The failure mechanism consists of a unit displacement $\delta = 1$ along the line BC (Fig. 6). The internal work done $W_1$, $W_2$ and $W_3$ from rupture along BC, CD and DE are

$$W_1 = \int_0^{l_{BC}} c_u(s) \mathrm{d}s \qquad W_2 = \int_0^{r_{CF}\left(\frac{\pi}{4}+\theta\right)} c_u(s) \mathrm{d}s \qquad W_3 = \int_0^{l_{DE}} c_u(s) \mathrm{d}s \tag{12}$$

where $c_u(s)$ is the undrained shear strength of clay as function of the distance $s$. $l_{BC}$, $r_{CF}$ and $l_{DE}$ are the lengths of BC, CD and DE.

The internal work from Prandl rupture in zone 2 is

$$W_4 = \int_0^{r_{CF}} \int_0^{\left(\frac{\pi}{4}+\theta\right)} c_u(s, \tau) \mathrm{d}s \mathrm{d}\tau$$

and the internal work from selfweight in zone 4 is

$$W_5 = (\gamma_s - \gamma_w) A_4 \sin \theta$$

where $A_4$ is the area of zone 4.

If $c_u$ is modelled as a stochastic variable the limit state function is written:

$$g(\mathbf{X}) = \min_{\theta} \{ W_1 + W_2 + W_3 + W_4 - W_5 - (F_G - F_U) \sin \theta - F_H \cos \theta \} \tag{13}$$
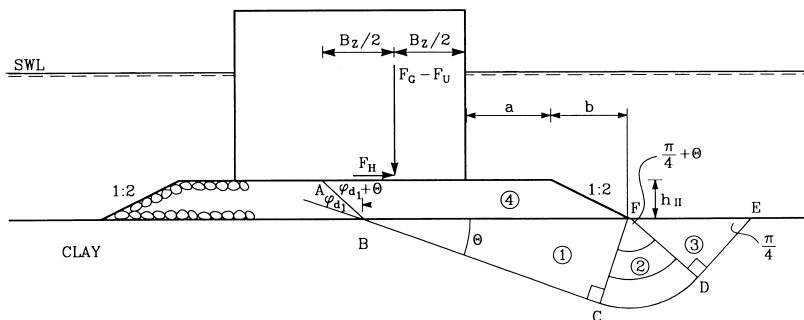


Fig. 6. Failure in rubble mound and in clay subsoil.

where $\theta \geqslant \max\left\{0, \tan^{-1}\left(\frac{h_{\mathrm{II}}}{B_z+a+b}\right) - \varphi_{d_1}\right\}$ is the angle of the rupture line.

If $c_u$ is modelled as a stochastic field the limit state function is written:

$$g(\mathbf{X}) = \min_{\theta}\left\{\mu_W + U\sigma_W - W_5 - (F_{\mathrm{G}} - F_{\mathrm{U}})\sin\theta - F_{\mathrm{H}}\cos\theta\right\} \qquad (14)$$

where

$U$    is a standard normally distributed stochastic variable: $N(0,1)$;

$\mu_W$    is the expected value of $W = W_1 + W_2 + W_3 + W_4$;

$\sigma_W$    is the standard deviation value of $W = W_1 + W_2 + W_3 + W_4$ which can be determined by numerical integration using Monte Carlo simulation and $\sigma_W^2 = \sum_{i=1}^{4}\sum_{j=1}^{4}\mathrm{Cov}[W_i, W_j]$ where $\mathrm{Cov}[W_i, W_j]$ is the covariance of $W_i$ and $W_j$.

For example, the expected value $E[W_1]$ and the covariance $\mathrm{Cov}[W_1, W_2]$ are obtained from

$$E[W_1] = \int_0^{l_{\mathrm{BC}}} E[c_u(s)]\mathrm{d}s$$

$$\mathrm{Cov}[W_1, W_2] = \int_0^{l_{\mathrm{BC}}}\int_0^{r_{\mathrm{CF}}(\pi/4+\theta)} C[c_u(s_1), c_u(s_2)]\mathrm{d}s_1\mathrm{d}s_2$$

where $C[c_u(s_1), c_u(s_2)]$ is the covariance function of $c_u$ at the positions corresponding to $s_1$ and $s_2$.

## 5. Example

The Niigata West breakwater in Japan is considered. The geometry is shown in Fig. 7. The caisson width is $B = 15$ m. The subsoil mainly consists of sand, but no



Fig. 7. Niigata West breakwater.

detailed information on the strength is available. Therefore both sand and clay subsoils are investigated in this example. For clay subsoil the mean value function and covariance function are assumed to be modeled by

$$E[c_u(x, z)] = c_{u0} + c_{u1}z$$

$$C[c_u(x_1, z_1), c_u(x_2, z_2)] = \sigma_{c_u}^2 \exp(-\alpha_c|z_1 - z_2|) \exp\left(-(\beta_c(x_1 - x_2))^2\right)$$
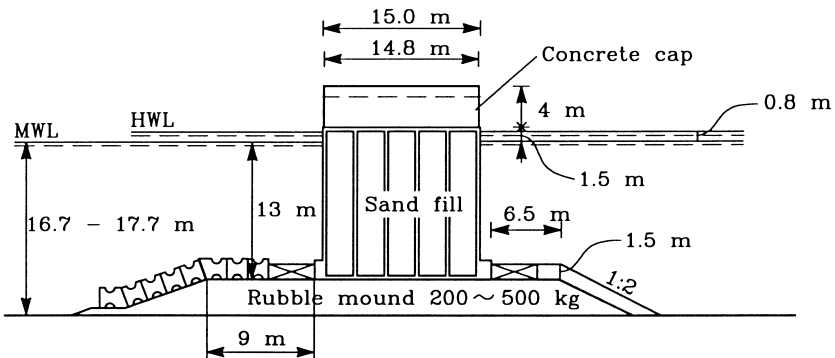
where $c_{u0} = 150$ kN/m$^2$ and $c_{u1} = 20$ kN/m$^2$/m model the expected value, $\sigma_{c_u} = 30$ kN/m$^2$ is the standard deviation and $\alpha_c = 0.33$ m$^{-1}$ and $\beta_c = 0.033$ m$^{-1}$ model the correlation.

The design significant wave height is 7.0 m. It is assumed that $N = 20$ data has been used to establish the statistical model for the significant wave height. If $\lambda = 1$, $\alpha = 1.5$ and $u = 2$ m the parameter $H'$ is calibrated such that the 98% fractile in the 1-year maximum wave distribution is 7.0 m [see (1)].

The model uncertainty related to the Goda wave load model can be significant. The uncertainty is modeled by multiplicative stochastic variables $U_{F_H}$ (horizontal force), $U_{M_H}$ (horizontal moment), $U_{F_U}$ (uplift force) and $U_{M_U}$ (uplift moment). The correlation coefficient is assumed to be 0.9 for $U_{F_H}$ and $U_{M_H}$ and 0.9 for $U_{F_U}$ and $U_{M_U}$. All other stochastic variables are independent. The reliability analysis is performed both for the case where model tests are performed and for the case where model tests are not performed.

The tidal elevation $\varsigma$ is modeled as a stochastic variable with distribution function

$$F_\varsigma(\varsigma) = \frac{1}{\pi} \arccos\left(-\frac{\varsigma}{\varsigma_0}\right)$$

where $\varsigma_0$ is the maximum tidal height.

The design lifetime is $T = 50$ years. The complete stochastic model is shown in Table 1.

Table 2 shows the results of a reliability analysis of the breakwater where the failure mode numbers refer to Section 4 and the Appendix. It is seen that the failure modes 1, 3, 7 (for sand subsoil) and 10 (for clay subsoil) are the most important. If no model tests are performed the system reliability index is $\beta_S = 0.86$ for sand subsoil and $\beta_S = 0.92$ for clay subsoil. If model tests are performed the system reliability indices increases to $\beta_S = 1.20$ for sand subsoil and $\beta_S = 1.29$ for clay subsoil. Since other civil engineering structures, e.g. bridges, usually have reliability index levels in the range from 3.7 to 5.2 (probabilities of failure from $10^{-4}$ to $10^{-7}$) the considered vertical wall breakwaters has a reliability level which is significantly smaller. However, this is also observed from reliability analyses for other breakwaters.

The results of sensitivity analyses are shown in Tables 3 and 4. The results in Table 3 show that if no model tests are performed the most important stochastic variables are $H_S$, $u$, $U_{F_H}$, $f$ (for sliding), $\varphi_1$ and $U$ (modeling the uncertainty in strength of clay subsoil). If model tests are performed then as expected the importance

Table 1
Statistical model for Niigata West breakwater[a,b]

| $i$ | $X_i$ | | Mean | Standard deviation | Distribution |
|---|---|---|---|---|---|
| 1 | $H_S$ | Significant wave height (m) | 3.4 | 1.2 | W |
| 2 | $u$ | Weibull parameter (m) | 2 | 0.46 | N |
| 3 | $U_{H_S}$ | model uncertainty on wave height | 1 | 0.05 | N |
| 4 | $\varsigma$ | Tidal elevation, maximum $\varsigma_0 = 1.5$ m | | | Cosine |
| 5 | $U_{F_H}$ | Model uncertainty horizontal force | 0.90 | 0.05/0.25 | N |
| 6 | $U_{F_U}$ | Model uncertainty uplift | 0.77 | 0.05/0.25 | N |
| 7 | $U_{M_H}$ | Model uncertainty horizontal moment | 0.81 | 0.10/0.40 | N |
| 8 | $U_{M_U}$ | Model uncertainty uplift moment | 0.72 | 0.10/0.37 | N |
| 9 | $\rho_c$ | Average density of caisson (t/m$^3$) | 2.23 | 0.11 | N |
| 10 | $\varphi_1$ | Effective friction angle — rubble mound | 35° | 3.5° | LN |
| 11 | $\psi_1$ | Angle of dilation — rubble mound | 25° | 2.5° | LN |
| 12 | $\varphi_2$ | Effective friction angle — sand subsoil | 30° | 3.0° | LN |
| 13 | $\psi_2$ | Angle of dilation — sand subsoil | 20° | 2.0° | LN |
| 14 | $U$ | Clay strength (auxiliary variable) | 1 | 0 | N |
| 15 | $f$ | Friction coefficient | 0.636 | 0.0954 | LN |

[a] For variables 5, 6, 7 and 8 the first value of the expected value is for model tests performed and the second number is for no model tests.
[b] W: Weibull, N: normal, LN: lognormal.

Table 2
Reliability indices for different failure modes[a]

| Failure mode | No model tests | Model test |
|---|---|---|
| 1 Rubble mound | 1.02 (1.54×10$^{-1}$) | 1.45 (7.35×10$^{-2}$) |
| 2 | 2.10 (1.79×10$^{-2}$) | 3.24 (5.98×10$^{-4}$) |
| 3 | 1.47 (7.08×10$^{-2}$) | 2.12 (1.70×10$^{-2}$) |
| 4 | 3.53 (2.08×10$^{-4}$) | 3.54 (2.00×10$^{-4}$) |
| 5 Sand subsoil | 2.12 (1.70×10$^{-2}$) | 3.24 (5.98×10$^{-4}$) |
| 6 | 1.32 (9.34×10$^{-2}$) | 2.14 (1.62×10$^{-2}$) |
| 7 | 1.09 (1.38×10$^{-1}$) | 1.51 (6.55×10$^{-2}$) |
| System sand subsoil | 0.86 (0.81) | 1.20 (10.88) |
| 8 Clay subsoil | 1.76 (3.92×10$^{-2}$) | 2.53 (5.70×10$^{-3}$) |
| 9 | 1.89 (2.94×10$^{-2}$) | 3.43 (3.02×10$^{-4}$) |
| 10 | 1.45 (7.35×10$^{-2}$) | 1.97 (2.44×10$^{-2}$) |
| System clay subsoil | 0.92 (0.82) | 1.29 (0.90) |

[a] The numbers in parentheses indicate the corresponding probability of failure.

of $U_{F_H}$ is decreased and the importance of $U$, $\rho_c$, $\varphi_1$ and $\varphi_2$ are increased. Especially the importance of the model uncertainty $U_{F_H}$ is decreased significantly when tests are performed.

In Table 4 so-called reliability elasticity coefficients $e_p = \frac{\mathrm{d}\beta}{\mathrm{d}p}\frac{p}{\beta}$ are shown. $p$ is a deterministic parameter, here the expected value for some of the stochastic variables.

Table 3
Importance factors $\alpha_i^2$: model tests performed/no model tests performed

| Variable | Failure mode 1 sliding | Failure mode 3 rubble mound | Failure mode 7 sand subsoil | Failure mode 10 clay subsoil |
|---|---|---|---|---|
| $H_S$ | 0.16/0.22 | 0.11/0.13 | 0.20/0.20 | 0.09/0.09 |
| $u$ | 0.20/0.27 | 0.14/0.15 | 0.23/0.24 | 0.12/0.12 |
| $U_{H_S}$ | 0.02/0.03 | 0.01/0.02 | 0.02/0.05 | 0.01/0.01 |
| $\varsigma$ | 0.00/0.00 | 0.00/0.02 | 0.00/0.00 | 0.00/0.00 |
| $U_{F_H}$ | 0.41/0.03 | 0.56/0.08 | 0.44/0.12 | 0.53/0.04 |
| $U_{F_U}$ | 0.01/0.00 | 0.02/0.01 | 0.02/0.01 | 0.01/0.00 |
| $U_{M_H}$ | — | — | 0.03/0.01 | 0.05/0.00 |
| $U_{M_U}$ | — | — | 0.00/0.00 | 0.00/0.00 |
| $\rho_c$ | 0.05/0.10 | 0.05/0.19 | 0.01/0.05 | 0.00/0.00 |
| $\varphi_1$ | — | 0.11/0.40 | 0.02/0.14 | 0.00/0.00 |
| $\psi_1$ | — | 0.00/0.00 | 0.00/0.00 | 0.00/0.00 |
| $\varphi_2$ | — | — | 0.03/0.18 | — |
| $\psi_2$ | — | — | 0.00/0.00 | — |
| $U$ | — | — | — | 0.19/0.74 |
| $f$ | 0.15/0.35 | — | — | — |

Table 4
Reliability elasticity coefficients $e_p = \frac{\mathrm{d}\beta}{\mathrm{d}p}\frac{p}{\beta}$ for expected value of some parameters: model tests performed/ no model tests performed

| Variable | Failure mode 1 sliding | Failure mode 3 rubble mound | Failure mode 7 sand subsoil | Failure mode 10 clay subsoil |
|---|---|---|---|---|
| $H_S$ | −0.39/−0.41 | −0.23/−0.17 | −0.40/−0.30 | −0.21/−0.15 |
| $u$ | −0.44/−0.45 | −0.25/−0.19 | −0.44/−0.33 | −0.22/−0.17 |
| $U_{F_H}$ | −2.07/−2.79 | −1.13/−1.70 | −0.89/−1.80 | −0.52/−0.62 |
| $U_{F_U}$ | −0.39/−0.49 | −0.19/−0.25 | 0.07/0.13 | −0.14/−0.20 |
| $U_{M_H}$ | — | — | −0.72/−1.14 | −0.59/−0.58 |
| $U_{M_U}$ | — | — | −0.29/−0.47 | −0.24/−0.24 |
| $\rho_c$ | 4.31/5.68 | 3.03/4.13 | 1.64/2.83 | 0.48/1.63 |
| $\varphi_1$ | — | 2.24/3.33 | 1.25/2.68 | 0.30/0.34 |
| $\psi_1$ | — | 0.21/0.19 | 0.13/0.24 | 0.03/0.04 |
| $\varphi_2$ | — | — | 1.53/3.05 | — |
| $\psi_2$ | — | — | 0.09/0.14 | — |
| $f$ | 2.52/3.43 | — | — | — |
| $U$ | — | — | — | 0.30/0.44 |
| $B$ | 2.94/1.70 | 2.43/1.52 | 2.25/2.25 | 1.52/0.95 |
| $T$ | −0.02/−0.27 | −0.01/−0.20 | −0.30/−0.29 | −0.01/−0.16 |

From Table 4 it is noted, that if the width of the caisson is increased by 1 m then the reliability indices are approximately increased by 10% and if the expected lifetime is decreased by 10 years the reliability indices are approximately increased by 1–4%.

## 6. Conclusion

Limit state functions are formulated for the most significant foundation failure modes for vertical wall breakwaters. The limit state functions are described using the upper bound theory of general plasticity theory assuming kinematically possible failure mechanisms. It is shown how the most critical failure modes can be modeled in a limit state function by minimizing the total virtual work with respect to the free parameters modeling the failure modes.

Further stochastic models for the main uncertainties related to wave loading and the geotechnical parameters related to sand and clay subsoil are presented. Based on these models it is shown how reliability analyses of vertical wall breakwaters can be performed using FORM and simulation. As an example a reliability analysis is performed for the geotechnical failure modes for the Niigata West breakwater in Japan. A reliability analysis is performed on the basis of the available limited information. The analysis shows that compared with other civil engineering structures the reliability level is significantly smaller.

## Acknowledgement

## Appendix. Limit state functions

### A.1. Failure in rubble mound — failure mode 4

The failure mechanism consists of a unit displacement $\delta = 1$ along line AB. The limit state function is written

$$g(\mathbf{X}) = \min_{\theta,\alpha}\left\{W_1 + W_2 + W_3 + (F_\mathrm{G} - F_\mathrm{U})\omega_\mathrm{1V} - F_\mathrm{H}\omega_\mathrm{1H}\right\} \qquad (\text{A1})$$

where $\omega_\mathrm{1V} = \sin(\varphi_{d_1} - \theta)/\cos\varphi_{d_1}$ and $\omega_\mathrm{1H} = \cos(\varphi_{d_1} - \theta)/\cos\varphi_{d_1}$.

$W_1$ is the work from the selfweight in zone 1 with area $A_1$:

$$W_1 = (\gamma_s - \gamma_w)A_1\omega_\mathrm{1V}$$

$W_2$ is the work from the selfweight in zone 2:

$$W_2 = (\gamma_s - \gamma_w)\omega_1 \frac{r_{CD}^2}{2\tan^2\varphi_{d_1} + 2}[\mathrm{e}^{\alpha\tan\varphi_{d_1}}\left(\tan\varphi_{d_1}\sin(\varphi_{d_1} - \theta + \alpha) - \cos(\varphi_{d_1} - \theta + \alpha)\right) - \left(\tan\varphi_{d_1}\sin(\varphi_{d_1} - \theta) - \cos(\varphi_{d_1} - \theta)\right)]$$

where $r_{CD}$ is the length of CD. $\alpha$ is shown in Fig. A1 and $\omega_1 = 1/\cos\varphi_{d_1}$.

$W_3$ is the work from the selfweight in zone 3 with area $A_3$:

$$W_3 = (\gamma_s - \gamma_w)A_3\omega_{3V}$$

where

$$\omega_{3V} = \frac{\sin(\varphi_{d_1} + \alpha - \theta)}{\cos\varphi_{d_1}} e^{\alpha\tan\varphi_{d_1}}$$

The following constraints to the minimization problem in (A1) are used:

$$0 \leqslant \theta$$

$$0 \leqslant \alpha \leqslant \theta$$

$$\beta + \alpha - \theta \ll 0, \quad \beta \text{ is defined in Fig. A1}$$

$$A_3 \geqslant 0$$

## A.2. Failure in rubble mound and sliding along top of subsoil (clay/sand) — failure modes 5 and 8

The failure mechanism consists of a unit displacement $\delta = 1$ along top of subsoil. For sand subsoil the limit state function is written (failure mode 5) (Fig. A2)

$$g(\mathbf{X}) = (\gamma_s - \gamma_w)A_1\tan\varphi_{d_2} + (F_G - F_U)\tan\varphi_{d_2} - F_H \tag{A2}$$

where $A_1$ is the area of zone 1.

For clay subsoil the limit state function is written (failure mode 8)

$$g(\mathbf{X}) = l_{BC}c_u - F_H \tag{A3}$$
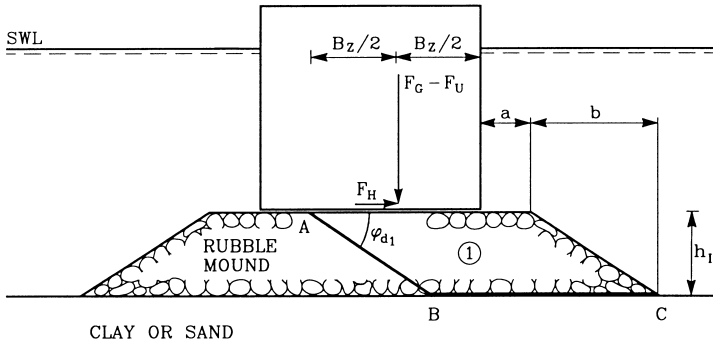


Fig. A1. Failure in rubble mound.

Fig. A2. Failure in rubble mound.

where $c_u$ is the undrained shear strength of clay and $l_{BC}$ is the length of BC.

## A.3. Failure in rubble mound and sand subsoil, failure mode 6

The failure mechanism consists of a unit displacement $\delta = 1$ along line AB. The limit state function is written

$$g(\mathbf{X}) = \min_{\theta} \left\{ W_1 + W_2 + W_3 + W_4 + (F_G - F_U)\omega_{1V} - F_H\omega_{1H} \right\} \tag{A4}$$

where $\omega_{1V} = \sin(\varphi_{d_1} - \theta)/\cos\varphi_{d_1}$ and $\omega_{1H} = \cos(\varphi_{d_1} - \theta)/\cos\varphi_{d_1}$.
$W_1$ is the work from the selfweight in zone 1 with area $A_1$:

$$W_1 = (\gamma_s - \gamma_w)A_1\omega_{1V}$$

$W_2$ is the work from the selfweight in zone 2 with area $A_2$ and $\omega_{2V} = \omega_{1V}$:

$$W_2 = (\gamma_s - \gamma_w)A_2\omega_{2V}$$

$W_3$ is the work from selfweight in zone 3:

$$W_3 = (\gamma_s - \gamma_w)\omega_1 \frac{r_{DF}^2}{2\tan^2\varphi_{d_2}+2}[e^{\theta_5\tan\varphi_{d_2}}\left(\tan\varphi_{d_2}\sin(\varphi_{d_1} - \theta + \theta_5) - \cos(\varphi_{d_1} - \theta + \theta_5)\right) - \left(\tan\varphi_{d_2}\sin(\varphi_{d_1} - \theta) - \cos(\varphi_{d_1} - \theta)\right)]$$

where $r_{DF}$ is the length of DF. $\theta_5$ is shown in Fig. A3 and $\omega_1 = 1/\cos\varphi_{d_1}$.
$W_4$ is the work from the selfweight in zone 4 with area $A_4$:

$$W_4 = (\gamma_s - \gamma_w)A_4\omega_{4V}$$

where

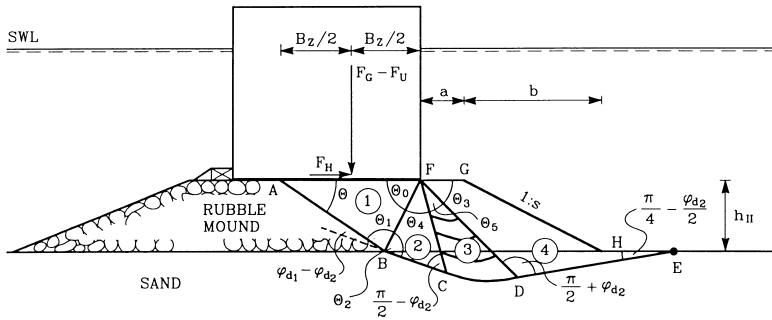$$\omega_{4V} = \frac{\sin(\varphi_{d_1} + \theta_5 - \theta)}{\cos\varphi_{d_1}}e^{\theta_5\tan\varphi_{d_2}}$$

Fig. A3. Failure in rubble mound.

The following constraints to the minimization problem are used:

$$\tan^{-1}\left(\frac{h_{\mathrm{II}}}{B_z + a + b}\right) \leqslant \theta \quad \text{rupture line should enter the subsoil}$$

$$\theta_1 \geqslant \frac{\pi}{2} - \varphi_{d_1}$$

$$A_2 \geqslant 0$$

### A.4. Failure in rubble mound and sand subsoil, failure mode 7

The failure mechanism consists of a unit displacement $\delta = 1$ along line AB. The limit state function is written:

$$g(\mathbf{X}) = \min_{\theta}\big\{W_1 + W_2 + W_3 + W_4 + W_5 + (F_{\mathrm{G}} - F_{\mathrm{U}})\omega_{1\mathrm{V}} - F_{\mathrm{H}}\omega_{1\mathrm{H}}\big\} \tag{A5}$$

where $\omega_{1\mathrm{V}} = \sin(\varphi_{d_1} - \theta)/\cos\varphi_{d_1}$ and $\omega_{1\mathrm{H}} = \cos(\varphi_{d_1} - \theta)/\cos\varphi_{d_1}$.
$W_1$ is the work from the selfweight in zone 1 with area $A_1$:

$$W_1 = (\gamma_s - \gamma_w)A_1\omega_{1\mathrm{V}}$$

$W_2$ is the work from the selfweight in zone 2 with area $A_2$ and $\omega_{2\mathrm{V}} = \omega_{1\mathrm{V}}$:

$$W_2 = (\gamma_s - \gamma_w)A_2\omega_{2\mathrm{V}}$$

$W_3$ is the work from selfweight in zone 3:

$$W_3(\gamma_s - \gamma_w)\omega_1 \frac{r_{DI}^2}{2\tan^2\varphi_{d_2} + 2}[\mathrm{e}^{\theta_5\tan\varphi_{d_2}}\big(\tan\varphi_{d_2}\sin(\varphi_{d_1} - \theta + \theta_5) - \cos(\varphi_{d_1} - \theta + \theta_5)\big) - \big(\tan\varphi_{d_2}\sin(\varphi_{d_1} - \theta) - \cos(\varphi_{d_1} - \theta)\big)]$$

where $r_{DI}$ is the length of DI. $\theta_5$ is shown in Fig. A4 and $\omega_1 = 1/\cos\varphi_{d_1}$.

$W_4$ is the work from the selfweight in zone 4 with area $A_4$:

$$W_4 = (\gamma_s - \gamma_w)A_4\omega_{4V}$$

where

$$\omega_{4V} = \frac{\sin(\varphi_{d_1} + \theta_5 - \theta)}{\cos\varphi_{d_1}} e^{\theta_5 \tan\varphi_{d_2}}$$

$W_3$ is the work from the selfweight in zone 3:

$$W_5 = (\gamma_s - \gamma_w)\omega_4 \frac{r_{GF}^2}{2\tan^2\varphi_{d_2} + 2}[e^{\theta_7 \tan\varphi_{d_2}}$$
$$\left(\tan\varphi_{d_2}\sin(\varphi_{d_1} + \theta_5 - \theta + \theta_7) - \cos(\varphi_{d_1} + \theta_5 - \theta + \theta_7)\right) -$$
$$\left(\tan\varphi_{d_2}\sin(\varphi_{d_1} + \theta_5 - \theta) - \cos(\varphi_{d_1} + \theta_5 - \theta)\right)]$$

where $r_{GF}$ is the length of GF. $\theta_7$ is shown in Fig. A4 and $\omega_4 = \omega_1 e^{\theta_5 \tan\varphi_{d_2}}$.

The following constraints to the minimization problem are used:

$$\tan^{-1}\left(\frac{h_{II}}{B_z + a + b}\right) \leqslant \theta \quad \text{rupture line should enter the subsoil}$$

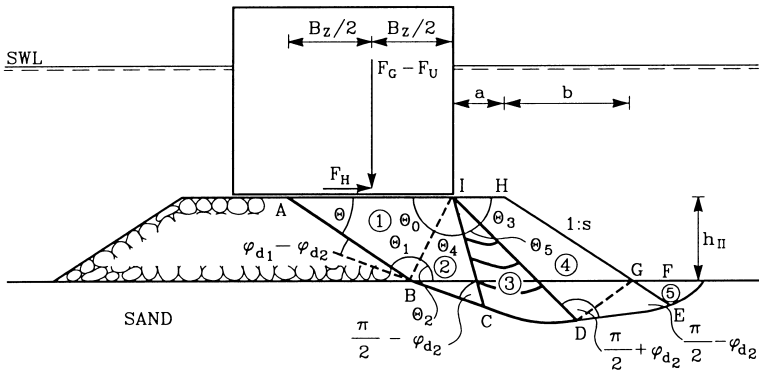$$\theta_1 \geqslant \frac{\pi}{2} - \varphi_{d_1}$$

$$A_2 \geqslant 0$$



Fig. A4. Failure in rubble mound.

## A.5. Failure in rubble mound and clay subsoil, failure mode 10

The failure mechanism consists of a unit rotation $\beta = 1$ about point D.

$W_1$ is the work from the selfweight in zone 1 with area $A_1$ where $l_{AE}$ is the length of AE and $x_D$ is shown in Fig. A5:

$$W_1 = (\gamma_s - \gamma_w) A_1 (x_D - \frac{2}{3} l_{AE})$$

$W_2$ is the work from the selfweight in zone 2 with area $A_2$:

$$W_2 = (\gamma_s - \gamma_w) A_2 \frac{1}{2} b$$

$W_3$ is the work from the selfweight in zone 3:

$$W_3 = (\gamma_s - \gamma_w) A_3 (\frac{1}{2} l_{BC} - \frac{2}{3} b)$$

The internal work from rupture along circle BC is

$$W_4 = r_{BD} \int_0^{2\alpha r_{BD}} c_u(s) \mathrm{d}s$$

where $r_{BD}$ is the length of BD, $\alpha$ is shown in Fig. A5 and $c_u(s)$ is the undrained shear strength of clay as function of distance $s$.

If $c_u$ is modelled as a stochastic variable the limit state function is written:

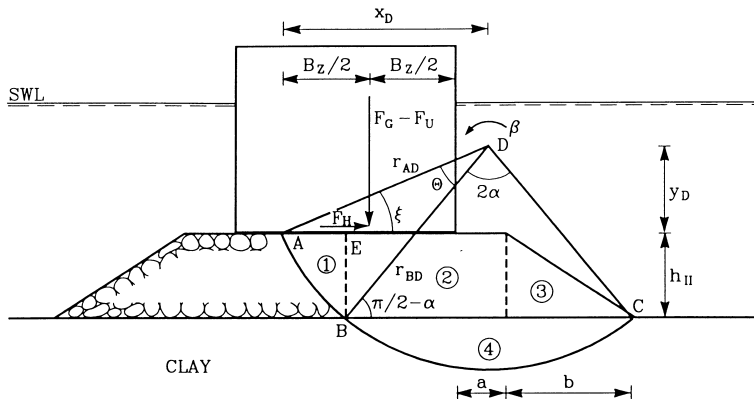$$g(\mathbf{X}) = \min_{x_D, y_D} \left\{ -W_1 - W_2 + W_3 + W_4 - (F_G - F_U)(x_D - \frac{1}{2} B_z) - F_H y_D \right\} \qquad \text{(A6)}$$



Fig. A5. Failure in rubble mound and in clay subsoil.

where $x_D$ and $y_D$ are the $x$- and $y$-coordinates of point D.

If $c_u$ is modelled as a stochastic field the limit state function is written:

$$g(\mathbf{X}) = \min_{x_D, y_D} \left\{ -W_1 - W_2 + W_3 + \mu_{W_4} + U\sigma_{W_4} - (F_G - F_U)(x_D - \frac{1}{2}B_z) - F_H y_D \right\}$$
(A7)

where

$U$ is a standard Normally distributed stochastic variable: $N(0,1)$

$\mu_{W_4}$ is the expected value of $W_4$ which can be determined by numerical integration.

$\sigma_{W_4}$ is the standard deviation value of $W_4$ which can be determined by numerical integration using Monte Carlo simulation.

The following constraints to the minimization problem are used:

$y_D \geqslant 0$

$\frac{B_z}{2} \leqslant x_D \leqslant B_z + a + b$

$r_{BD} \cos \alpha = y_D + h_{II}$

$\alpha \geqslant 0$

$\theta \geqslant 0.$

# References

[1] Burcharth HF. Identification of design tools for vertical wall breakwaters. PIANC PTC II Working Group 28, report by sub-group A, (1998).
[2] Sørensen CS, Ibsen, LB, Jakobsen, FR, Hansen A, Jakobsen KP. Bearing capacity of caisson breakwaters on rubble mounds. Annex IX of Foundation design of caisson breakwaters. Publication no. 198. Oslo: Norwegian Geotechnical Institute, 1996.
[3] Christiani E. Application of reliability in breakwater design. PhD thesis, Department of Civil Engineering, Aalborg University, 1997.
[4] Sørensen JD, Voortman H, Burcharth HF. Failure modes for vertical wall breakwaters. To be published in Final report, MAST III/PROVERBS project, 2000.
[5] Oumeraci H, Kortenhaus A. Wave impact loading — tentative formulae and suggestions for the development of final formulae. Proc. MAST III/PROVERBS workshop, Delft, September 1997.
[6] Goda Y. A new method of wave pressure calculation for the design of composite breakwater. Proc. 14th Int. Conf. Coastal Eng. Copenhagen, Denmark, 1974.
[7] Takayama T. Estimation of sliding failure probability of present breakwaters for probabilistic design. Report of Port and Harbor Research Institute, vol. 31(5), Yokosuka, Japan, 1992.
[8] Sørensen JD, Burcharth, HF. Implementation of safety in the design. Report of sub-group D, PIANC Working Group 28, 1998.
[9] Keaveny JM, Nadim, F, Lacasse, S. Autocorrelation function for offshore geotechnical data. Proc. ICOSSAR89, 1989. p. 263–70.

[10] Lindley DV. Introduction to probability and statistics from a Bayesian viewpoint, vols. 1 and 2. Cambridge: Cambridge University Press, 1976.

[11] Hansen B. Definition and use of friction angles. Proc. Int. Conf. VII ECSMFE, Brighton, UK, 1979.

[12] Madsen HO, Krenk S, Lind NC. Methods of structural safety. Prentice Hall, 1986.

[13] Ditlevsen O, Madsen HO. Structural reliability methods. Wiley, 1996.